Petrography and Geochemistry of Alkaline Basalts from the Sierra de Valle Fértil, Western Sierras Pampeanas, Argentina

B. Castro de Machuca[1], M. G. López[1,2], D. Morata[3], A. Conte-Grand[2], S. Pontoriero[2], J.P. Domínguez[2]
[1]CONICET- Argentina. E-mail: bcastro@unsj-cuim.edu.ar. Projects PIP09-0878 CONICET and 21/E896 CICITCA-UNSJ
[2]Instituto de Geología (INGEO), FCEFN, Universidad Nacional de San Juan. Av. Ignacio de la Roza y Meglioli, CP 5407 Rivadavia, San Juan, Argentina
[3]Departamento de Geología - Centro de Excelencia en Geotermia de los Andes (FONDAP-CEGA), Universidad de Chile, Santiago, Chile

Abstract. Alkaline basalts and trachybasalts ascribed to the latest stages of the Gondwanian orogenic cycle overlie the crystalline basement of the Sierra de Valle Fértil. These rocks have evolved from a MgO-rich primary magma and are the result of magmatic activity associated with intra-crustal rifting related to deep lithospheric fractures in the Western Sierras Pampeanas area.

Keywords: alkaline rocks, petrography, geochemistry, within-plate, Western Sierras Pampeanas

1 Introduction

Alkaline volcanic rocks of assumed Early Triassic age overlie and/or intrude the Proterozoic-Lower Palaeozoic high-grade crystalline basement of the Sierra de Valle Fértil, Western Sierras Pampeanas, province of San Juan, Argentina. The main outcrops are found on both sides of the Estancia Quiroga-Los Bretes depression, a NW-SE belt of *ca*. 30 km in length and up to 4 km wide limited by normal faults. Minor outcrops have been recognized within the range. These rocks evidence a compositional spectrum ranging from basalt and trachybasalt flows, associated with coeval intermediate phonolite and trachyte bodies, to alkaline rhyolite (Mirré, 1976). The mafic rocks predominate over the more silicic. Included amongst the first are the San Agustin Basalt (BSA, 30°38'3.2''S-67°28'28.5''W), the Usno Basalt (BU, 30°33'54.03''S-67°32'29.02''W), and the Los Molles-Los Bretes Trachybasalt (LM-LB, 30°46'01.71''S-67°27'17.96''W). The main geologic and petrographic features of these mafic rocks are here summarized. Also, major and trace element data and their relationship to the regional tectonic regime are presented.

2 Field Occurrence and Petrography

The lava flows have variable aerial extent. The BU covers an area of less than 0.03 km^2 whilst the LM-LB trachybasalt extends at about 5.7 km^2. The maximum thickness of basalt flows do not exceeds 6 m (Fig. 1a). At the BU and BSA exposures, two different flows are distinguished. An upper flow, relatively massive with narrowly spaced subhorizontal parting, rests on the top of a spheroidally weathered scoriaceous flow (Fig. 1b). The LM-LB trachybasalt shows poorly defined columnar jointing < 7 cm in diameter however wavy flow-like structures and parting are common. Fresh rocks are dark grey to black, but locally are extensively weathered to light grey, purplish grey, or rust orange. In hand specimens, they are typically dense, fine grained, and sparsely phyric to aphyric. The BU is strongly vesicular and shows numerous ovoid and elongated vesicles (Fig. 1c), whereas the BSA shows only local rounded to ovoid amygdales that reached up to 12 cm in diameter. Vesicles are not enough significant in the LM-LB trachybasalt. Most of the voids are empty, but some are filled with calcite and other secondary minerals (mostly zeolites, quartz, chalcedony, analcite, chlorite and celadonite).

The basalt flows do not exhibit uniform petrographic characteristics. The BSA consists of plagioclase (≈ 50%), olivine (≈ 20%), pyroxene (≈ 10%) and opaque minerals (mainly magnetite ≈ 20%). Both mafic minerals are present as subhedral to euhedral phenocrysts and microphenocrysts, while oriented plagioclase is restricted to the fine-grained intergranular- and intersertal groundmass. Olivine phenocrysts and microphenocrysts are colourless to pale grey and range between 0.08 mm and 1.7 mm in size, displaying seriate texture. Some of them are embayed (Fig. 2a). The larger grains are moderately fractured and show incipient replacement by iddingsite and rarer chloritization along fractures and crystal edges. Clinopyroxene (augite) occurs as colourless to light brownish subhedral to euhedral, twinned and sector-zoned phenocrysts with sieve texture up to 2.0 mm in length. Apatite, small nepheline crystals and interstitial glass, may be present in the matrix.

The BU is composed of essential plagioclase (≈ 70%) and microphenocrysts (≤ 0.3 mm) of subhedral to euhedral olivine (≈ 10%) typically embayed and in many places aligned, completely pseudomorphed by iddingsite. Scarce phenocrysts of euhedral twinned plagioclase up to 0.5 mm long are also present and set in the very fine-grained groundmass made up of aligned plagioclase laths with trachytic texture (Fig. 2b). The groundmass plagioclase is sodic labradorite to calcic andesine; the

phenocrysts are more calcic (labradorite).

In the LM-LB trachybasalt, plagioclase is the dominant constituent (70-75%). It occurs in two generations as larger subhedral to euhedral oligoclase phenocrysts (up to 4 mm in length), and as small tabular to elongated microlites of andesine in the groundmass with a noticeable subparallel alignment (trachytic texture). The groundmass texture is intergranular, but some brown interstitial devitrified glass can be seen. The phenocrysts show multiple twining, zoning and sieve-textured rims (Fig. 2c). Scarce microphenocrysts of completely altered olivine along with a high proportion (≈ 20%) of opaque minerals (mostly magnetite) and accessory apatite are scattered throughout the rock.

The BSA and BU are olivine and nepheline normative, consistent with the phenocryst mineralogy of Pl+Ol±Cpx, suggesting that these rocks have evolved in low pressure crystal equilibrium from MgO-rich primary magma.

3 Geochemistry

In terms of total alkalis *vs.* SiO_2 (Fig.3a), the studied rocks lie in the field of the alkaline magma series, ranging from olivine basalt-basanite (BU and BSA) to trachybasalt or mugearite (LM-LB). Major and trace element compositions vary somewhat, but are in the range expected for alkaline rocks.

The SiO_2 values range from 45-48.4 wt% in the basalts and from 50.8-51.8 wt% in the trachybasalt. The MgO content of the BSA and BU ranges from 3.5-7.12 wt% and from 2.07-1.13 wt%, respectively, whilst it varies from 0.8-3.46 wt% in the LM-LB. The total FeO content varies between 12.2-13 wt% in the BSA, from 11.8-12.9 wt% in the BU and from 11-11.9 wt% in the LM-LB. BSA has Na_2O and K_2O averages of 4.34 and 1.54 wt%, BU 3.88 and 3.70 wt%, and LM-LB 5.12 and 2.90 wt%, respectively. In Harker diagrams MgO, CaO, Na_2O and TiO_2 show negative correlations with SiO_2 whilst Al_2O_3 and K_2O show positive correlation. Trace element contents such as Cr, Ni and V decrease with increasing SiO_2 content while Rb shows a positive correlation with silica.

The BSA has moderate to high Ni and Cr contents. Ni average is 122 ppm and Cr average content is 200 ppm. These values are significantly lower for the BU (Ni 23 wt% and Cr < 10 wt% averages) and for the LM-LB (Ni 18 wt% and Cr 33.7 wt% averages). Rb content in the BSA is relatively low, with an average of 13 ppm, but it increases in the LM-LB (33.15 ppm average) and in the BU (39.5 ppm average). Sr content in the basalts ranges from 711 to 1600 ppm (967 ppm average) and, in the LM-LB trachybasalt from 843 to 901 ppm (858.5 ppm average). The BSA, BU and LM-LB have average Zr contents of 214, 274 and 316 ppm, respectively. Nb values range between 50.8 to 67.6 ppm (57.4 ppm average). The averages of Zr/Nb ratio are 3.8, 5.0 and 5.3 for the BSA, BU and LM-LB, respectively. The Y content for all these rocks shows a very limited variation from 23.1 to 31.8 ppm (28.2 ppm average).

Spiderdiagrams for the basalts and the trachybasalt (Fig. 3b) show identical pattern with a peak at Nb-Ta. Nevertheless, BU is relatively depleted in Rb and K respect to the other analyzed rocks. In the chondrite-normalized REE diagram (Fig. 3c) light-REE are strongly enriched while heavy-REE abundances are about 7 to 15 times the chondritic values, suggesting the presence of garnet as residual phase in the source.

Several geochemical discrimination diagrams were applied in the interpretation of the tectonic setting of these rocks. In the Zr *vs*. Zr/Y diagram (Fig. 3d) all the samples fall within the intraplate basalt field. This is further supported by the Zr-Ti/100-Y*3 and Zr/4-Nb*2-Y diagrams (not shown). Moreover, in the La/10-Y/15-Nb/8 diagram (Fig. 3e) all samples are plotted in the field of alkaline basalts of continental intraplate (rift) setting.

Preliminary Considerations

In spite of the absence of radiometric age determinations of the alkaline volcanic activity in the area, it has been ascribed to the latest stages of the Gondwanian orogenic cycle (Early Triassic) characterized by active extensional faulting, development of sedimentary rift basins, and non-orogenic magmatism along the continental margin of Gondwana. The Triassic rift system has a general NW-SE trend controlled by basement fabrics. The BSA, BU and LM-LB are located along the margin of the uplifted eastern basement block of the Sierra de Valle Fértil following such broad structural trend, and are closely related to deep lithospheric fractures. The studied volcanic rocks would then be the result of intraplate magmatic activity associated with intra-crustal rifting.

References

Cabanis, B., Lecolle, M., 1989. Le diagramme La/10-Y/15-Nb/8; un outil pour la discrimination des series volcaniques et la mise en evidence des processus de melange et/ou de contamination crustale. Comptes Rendus de l'Academie des Sciences, Serie 2, Mecanique, Physique, Chimie, Sciences de l'Univers, Sciences de la Terre, 309: 2023-2029.

Irvine, T., Baragar, W. 1971. A guide to the chemical classification of the common volcanic rocks. Canadian Journal of Earth Sciences 8: 523-548.

Cox, K.G., Bell, J.D., Pankhurst, R.J., 1979. The Interpretation of Igneous Rocks. Allen and Unwin, London, 450p.

Mirré, J.C., 1976. Descripción Geológica de la Hoja 19e, Valle Fértil, Provincias de San Juan y La Rioja. Servicio Geológico Nacional, Boletín 147: 1-70. Buenos Aires.

Nakamura, N. 1974. Determination of REE, Ba, Fe, Mg, Na and K in carbonaceous and ordinary chondrites. Geochimica et Cosmochimica Acta 38: 757-775.

Pearce, J.A., Norry, M.L., 1979. Petrogenetic implications of Ti, Zr, Y, and Nb variations in volcanic rocks. Contrib. Mineral. Petrol. 69: 33-47.

Thompson, R.N., 1982. Magmatism of the British Tertiary Volcanic Province. Scottish Journal of Geology 18: 49-107.

Figure 1. a) LM-LB trachybasalt flow, b) lower scoriaceous and upper massive basalt flows (BU), c) Vesicular texture in the BU.

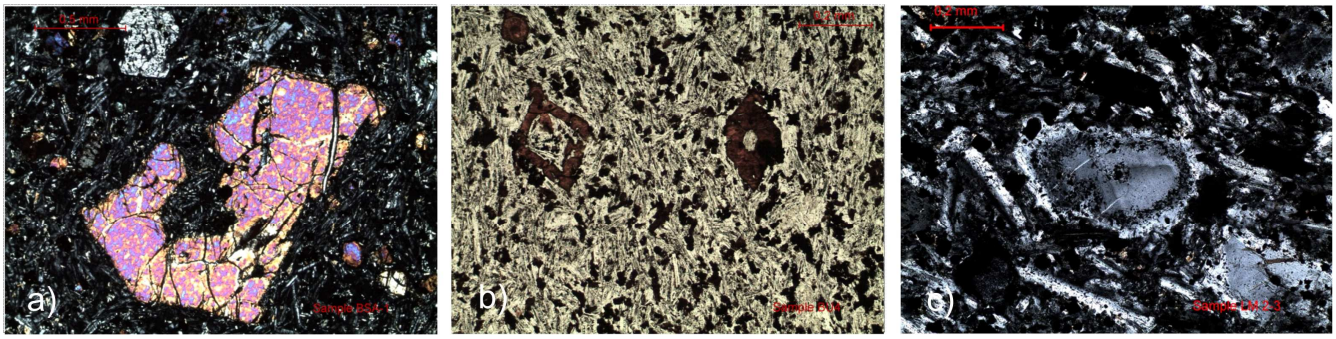

Figure 2. a) Embayed olivine phenocryst (NX), b) olivine microphenocrysts fully replaced by iddingsite in a groundmass of plagioclase laths and opaques (N//), c) zoned and sieve-textured plagioclase phenocrysts in a matrix of similar composition (NX).

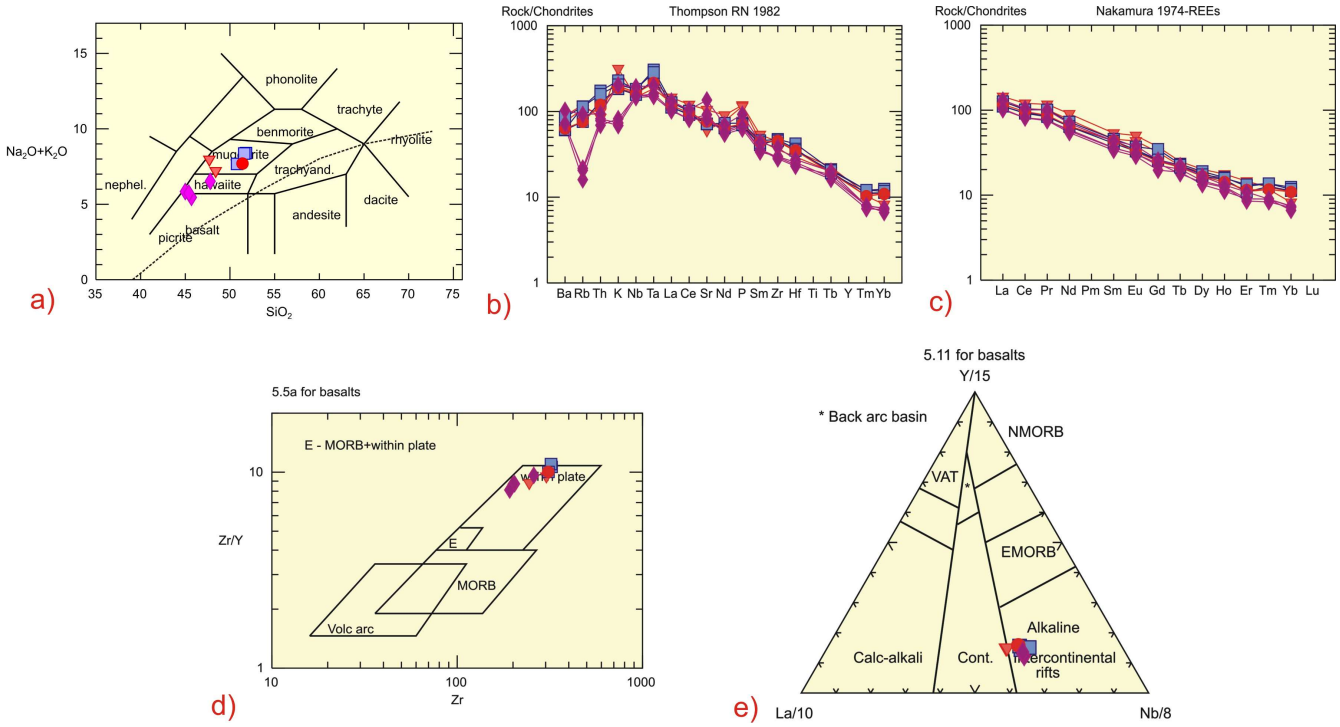

Figure 3. a) Classification diagram (Cox *et al.*, 1979). Also shown is the dashed line dividing subalkaline and alkaline fields (Irvine & Baragar, 1971), b) multi-element diagram normalized to chondrite (Thompson, 1982), c) REE diagram normalized to chondrite (Nakamura, 1974), d) Zr-Zr/Y diagram (Pearce & Norry, 1979), e) La/10-Y/15-Nb/8 diagram (Cabanis & Lecolle, 1989). BSA: rhombus, BU: triangle, LM-LB: square and circle.